

Estimating the $(\text{CO})_5\text{Cr}(\eta^2\text{-benzene})$ bond dissociation enthalpy: reaction of the $(\text{CO})_5\text{Cr}(\eta^2\text{-benzene})$ complex with a series of $(\text{CH}_3)_n\text{THF}$ ($n = 0, 1, 2,$ and 4) ligands

Ashfaq A. Bengali* and Trent F. Stumbaugh

Department of Chemistry, Dickinson College, Carlisle, PA 17013, USA.

E-mail: bengali@dickinson.edu

Received 25th October 2002, Accepted 18th November 2002

First published as an Advance Article on the web 2nd January 2003

The displacement of the benzene ligand from the photolytically generated $(\text{CO})_5\text{Cr}(\eta^2\text{-benzene})$ complex by THF and a series of methyl substituted $(\text{CH}_3)_n\text{THF}$ ($n = 1, 2,$ and 4) ligands was studied using the technique of laser flash photolysis. The data suggest that two independent pathways (D and I_d) contribute to the overall displacement of the benzene solvent from the Cr center. The contribution of the I_d pathway increases as the steric bulk of the Me_nTHF ligand is reduced from Me_4THF to MeTHF . The activation enthalpy of $11.4 \pm 1.1 \text{ kcal mol}^{-1}$ obtained when the entering ligand is Me_4THF is considered to be a lower estimate of the $(\text{CO})_5\text{Cr}(\eta^2\text{-benzene})$ bond dissociation enthalpy. A detailed energetic profile of the substitution reaction is presented.

Introduction

It is well established that photolysis of transition metal carbonyl complexes, $\text{M}(\text{CO})_n$, with UV light results in the dissociation of a metal–carbonyl bond.^{1–5} When the photolysis is carried out in condensed phase, the resulting coordinatively unsaturated metal complex reacts rapidly with the solvent to form the solvated complex $\text{M}(\text{CO})_{n-1}(\text{solvent})$.⁶ For example, photolysis of $\text{Cr}(\text{CO})_6$ in solution phase results in the formation of the $\text{Cr}(\text{CO})_5(\text{solvent})$ complex within picoseconds of CO loss.^{4,7}



The lifetime of the solvated complex is a function of the metal–solvent bond strength and can vary from nanoseconds to several minutes depending on the identity of the solvent. In weakly coordinating solvents like perfluoromethylcyclohexane (PFC), $\text{Cr}(\text{CO})_5(\text{PFC})$ has a lifetime of nanoseconds⁸ while in a strongly coordinating solvent like tetrahydrofuran (THF), the corresponding $\text{Cr}(\text{CO})_5(\text{THF})$ complex can exist for several minutes.⁹

Coordinatively unsaturated transition metal complexes are often implicated as intermediates in a variety of chemical reactions and therefore establishing the strength of the metal–solvent interaction in such complexes is important to a full understanding of the reaction mechanisms.¹⁰ In general two methods have been used to characterize the strength of this important interaction: kinetic studies which yield activation parameters proportional to the metal–solvent bond strength, and thermodynamic measurements using photoacoustic calorimetry (PAC).^{6,11–23} Quite often the values obtained by the two methods differ by several kcal mol^{-1} . For example, the $(\text{CO})_5\text{W}$ –solvent (solvent = heptane, cyclohexane) bond strengths obtained by studying the substitution kinetics of the solvated complex were approximately 6 kcal mol^{-1} lower than those obtained by PAC.¹³ The difference between the two numbers was attributed to partial solvation of the transition state by the alkane solvent in the kinetic study. It should also be noted that early measurements using PAC did not account for reaction volumes and the values reported for the metal–solvent bond strengths are likely too high.²² However, in some cases the two methods yield similar values as was the case for the $\text{CpMn}(\text{CO})_2$ –THF bond strength determination where both techniques yielded a value of $24 \pm 2 \text{ kcal mol}^{-1}$.^{17,23} The relationship between metal–solvent bond strengths obtained by kinetic methods and those determined by thermochemical measure-

ments is not yet well established and clearly more studies are required.

A case where there is disagreement between kinetic and thermodynamic measurements regarding the value of a metal–solvent bond strength is the $(\text{CO})_5\text{Cr}(\text{bz})$ ($\text{bz} = \text{benzene}$) complex. This complex is easily generated by photolysis of $\text{Cr}(\text{CO})_6$ in benzene solvent and involves coordination of the benzene molecule to the Cr center in an η^2 fashion.^{15,24} The strength of the Cr–bz interaction has been estimated using kinetic methods in both the condensed and gas phases. Dobson and co-workers studied the displacement of benzene from $(\text{CO})_5\text{Cr}(\text{bz})$ by piperidine and obtained an upper limit of $9.4 \pm 0.1 \text{ kcal mol}^{-1}$ for the Cr–bz bond strength.¹⁵ The reaction of $(\text{CO})_5\text{Cr}(\text{bz})$ with CO has also been studied in the gas phase and two independent kinetic studies obtained estimates of 9.2 ± 0.8 and $13.7 \pm 0.8 \text{ kcal mol}^{-1}$ for the Cr–benzene bond strength.^{12,25} Except for the $13.7 \text{ kcal mol}^{-1}$ estimate these numbers are considerably lower than the thermodynamic determination of $14.4 \pm 2.0 \text{ kcal mol}^{-1}$ for the Cr–benzene bond strength obtained by PAC studies.²⁶

In this paper we report the results of a kinetic study in which the benzene solvent is displaced from $\text{Cr}(\text{CO})_5(\text{bz})$ by a series of methyl substituted THF ligands; tetrahydrofuran (THF), 2-methyltetrahydrofuran (MeTHF), 2,5-dimethyltetrahydrofuran (Me_2THF), and 2,2,5,5-tetramethyltetrahydrofuran (Me_4THF). This system is a good test case for understanding the relationship between the kinetic and thermodynamic methods used to obtain weak metal–solvent bond strengths. Displacement of the benzene solvent from $(\text{CO})_5\text{Cr}(\text{bz})$ by some ligands has been shown to proceed through a dissociative process.¹⁵ Thus, activation parameters for the $(\text{CO})_5\text{Cr}(\text{bz}) \rightarrow (\text{CO})_5\text{Cr} + \text{bz}$ reaction are accessible in some cases. Furthermore, since the reaction of $\text{Cr}(\text{CO})_5$ with benzene proceeds with a negligible activation barrier ($< 2 \text{ kcal mol}^{-1}$),^{12,25} it should be possible to obtain reliable estimates of the $(\text{CO})_5\text{Cr}$ –bz bond strength by this kinetic method. As noted earlier, one such study yielded a value of $9.4 \pm 0.1 \text{ kcal mol}^{-1}$ in the condensed phase, about 5 kcal mol^{-1} lower than the PAC estimate. Presumably, the discrepancy between the two numbers is due to residual bonding between the $\text{Cr}(\text{CO})_5$ fragment and benzene in the transition state resulting in a lower estimate by the kinetic study.¹⁵ We were interested to see if we could access a more “dissociative” transition state by systematically increasing the steric bulk of the entering ligand. The steric constraints would then require the $(\text{CO})_5\text{Cr}$ –bz bond to be almost fully cleaved before the incoming sterically hindered ligand could bind to the Cr center. Thus, we were interested to see if better agreement between the

thermodynamic and kinetic estimates of the Cr–bz bond strength could be obtained. While addition of methyl groups to the THF ligand will make it a stronger σ donor, previous studies by Schultz and Krishnan²⁷ suggest that the reactivity of $\text{W}(\text{CO})_5(\text{cyclohexane})$ with $(\text{CH}_3)_n\text{THF}$ can be explained entirely by steric effects. By analogy, the electronic effect of increasing methyl substitution on the reactivity of the $(\text{CH}_3)_n\text{THF}$ ligands with $(\text{CO})_5\text{Cr}(\text{bz})$ is expected to be small. The results presented in this paper suggest that while this chemical system displays mechanistic complexity, the overall data present a clear and internally consistent account of the displacement of benzene from $\text{Cr}(\text{CO})_5(\text{bz})$ by Me_nTHF ligands.

Experimental

The time-resolved uv-vis absorption apparatus used in this study is briefly described here. Photolysis of the $\text{Cr}(\text{CO})_6$ solution was carried out using the 336 nm output of a nitrogen laser (Laser Science, 200 $\mu\text{J}/\text{pulse}$, 10 ns pulse width). The resulting transients were monitored using uv-vis light from a 150 W Xe arc lamp (Xenon Corporation). The light from the arc lamp was focused through the photolysis solution and onto the entrance slit of a 0.125 m monochromator (Jobin-Spex H-10, 8 nm band pass) which was used to identify the absorbing wavelength of the transient species. To prevent photolysis of the $\text{Cr}(\text{CO})_6$ solution by the Xe arc lamp, a 370 nm long bandpass filter (CVI Optics) was placed in front of the probe light. The solution temperature was controlled (± 0.1 °C) by using a water circulator (Fisher Scientific, 1016 S) and a jacketed quartz (1×1 cm) fluorescence cuvette.

The concentration of $\text{Cr}(\text{CO})_6$ in the photolysis solutions was $\approx 3\text{mM}$. All runs were carried out under pseudo first-order conditions with the concentration of the Me_nTHF ligand at least 10 times that of $(\text{CO})_5\text{Cr}(\text{bz})$. The decay of the absorbance due to the $(\text{CO})_5\text{Cr}(\text{bz})$ complex was monitored at 520 nm and the growth of the product $(\text{CO})_5\text{Cr}(\text{Me}_n\text{THF})$ complexes was observed at 420 nm. These wavelengths were chosen to minimize the overlap between the absorption bands of the reactant and product. Signals were averaged over 100–150 laser shots. The reactant and product time profiles showed exponential decays and growths, respectively. The observed rate constants (k_{obs}) reported in this paper were obtained by fitting the first order decay of the reactant to a single exponential function. In nearly all cases the fits had correlation coefficients of ≥ 0.99 . Rate constants were determined by least-squares fits to the concentration dependence of k_{obs} and are reported with 1σ uncertainties. The error in the activation parameters obtained from Eyring plots are at the 95% confidence level and were obtained from a linear least-squares fit.

Benzene (bz) and heptane (Aldrich or Acros) solvents used in the experiment were dried over CaH_2 and were of 99%+ purity. Tetrahydrofuran (THF), 2-methyltetrahydrofuran (MeTHF), 2,5-dimethyltetrahydrofuran (Me₂THF), and 2,2,5,5-tetramethyltetrahydrofuran (Me₄THF) were also dried over CaH_2 and were of 99% purity except Me₄THF which had a stated purity of 98% (Aldrich or Acros). The Me₂THF solvent was a mixture of *cis* and *trans* isomers. Chromium hexacarbonyl (Aldrich) was used as received. All manipulations were done under an Ar atmosphere.

Results

(a) L = THF

As shown in Fig. 1, photolysis of a 3 mM benzene solution of $\text{Cr}(\text{CO})_6$ containing 0.12 M THF results in the formation of a transient species absorbing at 520 nm which undergoes a first order decay. A species absorbing at 420 nm is observed to grow in at the same rate. A clean isosbestic point is observed at 483 nm indicating the conversion of the reactant to a single

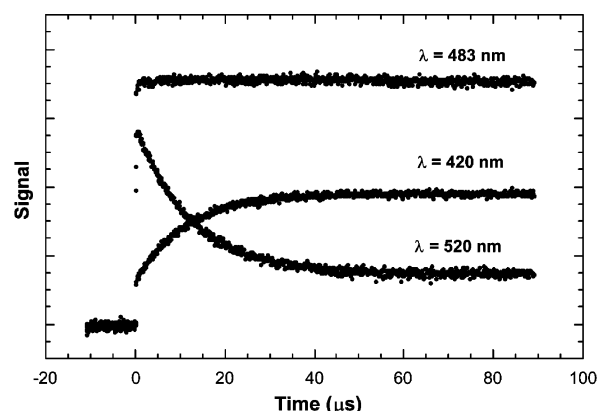


Fig. 1 Kinetic traces obtained upon photolysis of a 3 mM benzene solution of $\text{Cr}(\text{CO})_6$ with 0.12 M THF at 293 K. The decay of the $(\text{CO})_5\text{Cr}(\text{bz})$ complex and the growth of the $(\text{CO})_5\text{Cr}(\text{THF})$ product was monitored at 520 and 420 nm, respectively. The 520 nm reactant absorbance does not go down to the baseline because of overlap with the product absorption. An isosbestic point was observed at 483 nm indicating conversion of the $(\text{CO})_5\text{Cr}(\text{bz})$ complex to a single product.

product. By analogy with previous studies, the species absorbing at 520 nm is assigned to the $(\text{CO})_5\text{Cr}(\text{bz})$ complex¹⁵ and the product is the well known $(\text{CO})_5\text{Cr}(\text{THF})$ complex.⁹

The observed rate constant (k_{obs}), obtained by fitting the decay of the $(\text{CO})_5\text{Cr}(\text{bz})$ complex to a single exponential function, shows a linear dependence on the concentration of THF (Fig. 2). Such a variation of k_{obs} with THF concentration is

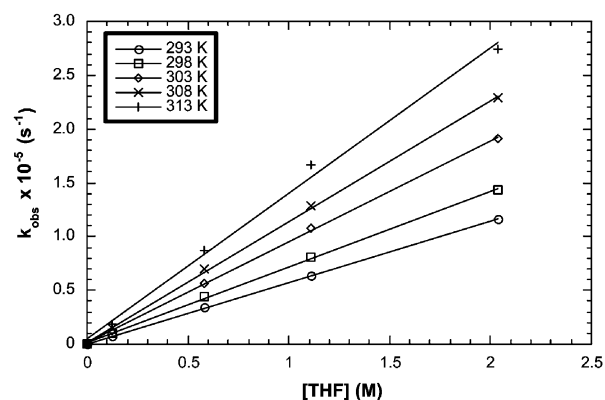
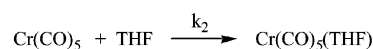
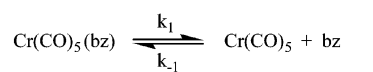
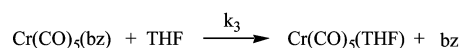


Fig. 2 Plot of k_{obs} vs. THF concentration from 293 to 313 K.

consistent with both a dissociative (Scheme 1) and interchange mechanism (Scheme 2) of benzene displacement from the Cr center.



Scheme 1



Scheme 2

Assuming a steady state concentration of the $\text{Cr}(\text{CO})_5$ complex, the observed rate for the dissociative mechanism shown above is:

$$k_{\text{obs}} = \frac{k_1 k_2 [\text{THF}]}{k_{-1} [\text{bz}] + k_2 [\text{THF}]} \quad (1)$$

If $k_{-1}[\text{bz}] \gg k_2[\text{THF}]$, a plot of k_{obs} vs. $[\text{THF}]$ will be linear with a slope of k' where

$$k' = \frac{k_1 k_2}{k_{-1}[\text{bz}]} \quad (2)$$

A linear dependence of k_{obs} on $[\text{THF}]$ is also expected if the displacement of benzene proceeds *via* a simple interchange pathway with a single transition state. In this case

$$k_{\text{obs}} = k_3[\text{THF}] \quad (3)$$

Previous studies have shown that the displacement of benzene from the Cr center follows a primarily dissociative path when $L = \text{piperidine}$ and 1-hexene while when $L = \text{pyridine}$, there is evidence for the involvement of an interchange step as well.¹⁵ In the case of THF, the available data does not allow us to unambiguously determine the mechanism of benzene displacement from the Cr center. It should be noted, however, that k_{obs} appears to be a function of benzene concentration since experiments where the benzene concentration was reduced by adding heptane as the diluent resulted in an increase in the observed rate implying the presence of a dissociative contribution to the overall mechanism. The activation parameters derived from an Eyring analysis using the slope of the k_{obs} vs. $[\text{THF}]$ plots yield values of $\Delta H^\ddagger = 7.5 \pm 0.5 \text{ kcal mol}^{-1}$ and $\Delta S^\ddagger = -11.4 \pm 1.8 \text{ e.u.}$ While it is difficult to analyze these values since the substitution mechanism is unclear, the activation enthalpy of $7.5 \text{ kcal mol}^{-1}$ is significantly lower than the estimates for the $(\text{CO})_5\text{Cr}-\text{bz}$ bond dissociation enthalpy which range from 9.2 ± 0.1 to $14.4 \pm 2.0 \text{ kcal mol}^{-1}$. Thus, the activation parameters suggest that the substitution of benzene from the $(\text{CO})_5\text{Cr}(\text{bz})$ complex by THF proceeds through a pathway that does not include complete Cr–bz bond dissociation in the transition state.

(b) $L = \text{MeTHF}$

As mentioned above, the rate of the substitution reaction exhibits a dependence on the concentration of benzene. Since addition of increasing amounts of ligand necessarily alters the concentration of benzene, it can be difficult to separate out the effect of ligand and benzene concentration on the rate of the reaction. Thus, in an effort to clarify the substitution mechanism, experiments were conducted using heptane as a diluent to keep the concentration of benzene constant as the MeTHF concentration was varied. In this experiment, heptane can be considered an “inert” solvent since the known $\text{Cr}(\text{CO})_5(\text{hep})$ complex is almost 1000 times more reactive than $(\text{CO})_5\text{Cr}(\text{bz})$.^{6,28} Thus, while photolysis of $\text{Cr}(\text{CO})_6$ in the mixed solvent will initially yield both the $\text{Cr}(\text{CO})_5(\text{hep})$ and $\text{Cr}(\text{CO})_5(\text{bz})$ complexes, the $\text{Cr}(\text{CO})_5(\text{hep})$ complex is expected to rapidly convert to the benzene complex within the “dead time” ($\approx 1 \mu\text{s}$) of the present experiment. In these experiments, the $\text{Cr}(\text{CO})_5(\text{hep})$ complex was not observed directly. However, as discussed later, the participation of the $\text{Cr}(\text{CO})_5(\text{hep})$ complex as an intermediate in the substitution reaction is quite likely. This mixed solvent experiment results in an increase in the observed rate since $[\text{bz}]$ is held at a lower value than in the pure solvent. A similar experiment was attempted for THF and while the rate did change, the reaction was too fast to measure reliably. It should be noted that the use of heptane as the diluent should not drastically effect the solvent characteristics since both heptane and benzene are non-polar and have similar viscosities.²⁹

The concentration of benzene was held constant at 2.8 M and the observed rate constant was obtained over a wide range of MeTHF concentrations. As shown in Fig. 3, the observed rate constant does not exhibit a linear dependence on MeTHF concentration. The curvature of the k_{obs} vs. L plots suggests

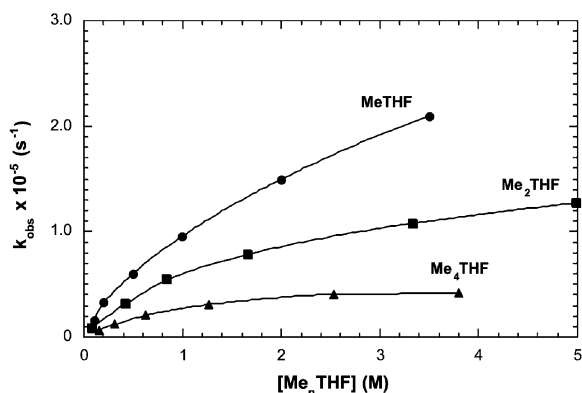


Fig. 3 A plot of k_{obs} vs. $[\text{Me}_n\text{THF}]$ at 293 K. The concentration of benzene is held constant at 2.8 M in all the runs. The solid line is a smooth interpolation between the data points and does not represent a fitted curve. Notice that at high $[\text{Me}_n\text{THF}]$ the observed rate appears to continue rising in the case of MeTHF and Me₂THF, but approaches a limiting value for Me₄THF.

that the overall substitution mechanism includes the presence of consecutive steps where at least one of these steps is reversible. A more complete discussion of the mechanism is presented later.

(c) $L = \text{Me}_2\text{THF}$ and Me_4THF

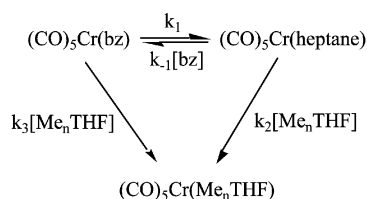
As with MeTHF, mixed solvent experiments with $L = \text{Me}_2\text{THF}$ and Me_4THF also show that k_{obs} does not exhibit a linear dependence on ligand concentration (Fig. 3). Because of the steric bulk of the Me₄THF ligand, the corresponding $(\text{CO})_5\text{Cr}(\text{Me}_4\text{THF})$ product complex is expected to have a short lifetime and there is a possibility that its formation is reversible. To ensure that the $(\text{CO})_5\text{Cr}(\text{Me}_4\text{THF})$ complex was stable on the timescale of the experiment, we also photolyzed a solution of $\text{Cr}(\text{CO})_6$ in neat Me₄THF to generate $(\text{CO})_5\text{Cr}(\text{Me}_4\text{THF})$. While the $(\text{CO})_5\text{Cr}(\text{bz})$ complex is stable for $\sim 1 \text{ ms}$ at 30 °C, the $(\text{CO})_5\text{Cr}(\text{Me}_4\text{THF})$ complex appeared stable for $>10 \text{ ms}$. Thus, we assume that formation of $(\text{CO})_5\text{Cr}(\text{Me}_4\text{THF})$ is irreversible on the timescale of the present experiment.

Discussion

The overall rate of the reaction between $(\text{CO})_5\text{Cr}(\text{bz})$ and Me_nTHF decreases as n increases from 0 to 4. A plausible mechanism for the substitution of benzene by the Me_nTHF ligands must take into account the following observations. (1) A plot of the observed rate vs. Me_nTHF concentration shows significant curvature. (2) The reaction rate depends upon the identity of the entering ligand such that the rate constants at high ligand concentration are different. (3) The reaction rate shows an inverse dependence on the concentration of benzene solvent. On the basis of these observations we can immediately rule out both a simple interchange reaction with a single transition state (Scheme 2) and a purely dissociative mechanism for the substitution of benzene by Me_nTHF (Scheme 1). The observed rate would show a linear dependence on $[\text{Me}_n\text{THF}]$ if the substitution reaction were interchange [eqn. (3)]. While a dissociative mechanism would yield a curved k_{obs} vs. $[\text{Me}_n\text{THF}]$ plot, the value of the limiting rate constant (k_1 in Scheme 1) would not depend on the identity of the incoming ligand as is clearly the case here (see Fig. 3).

While the experimental results rule out the presence of either a pure dissociative or interchange mechanism, they are consistent with the possibility that *both* pathways contribute to the overall substitution mechanism. Indeed, as noted earlier, it has previously been observed that both reaction channels (Schemes 1 and 2) contribute towards the displacement of bz from $\text{Cr}(\text{CO})_5(\text{bz})$ by pyridine. If both pathways are operative in the

substitution reaction, then the overall mechanism may appropriately be described as shown in Scheme 3.



Scheme 3

Since the reactions were conducted in mixed solvent using heptane as the diluent, it is reasonable to suggest the presence of the solvent stabilized $\text{Cr}(\text{CO})_5(\text{hep})$ complex as an intermediate in this reaction mechanism since it is a known species and has been observed previously.⁶ Thus, according to the classical Langford–Gray definition, the two contributing pathways, k_1 and k_3 shown in Scheme 3 may be formally classified as dissociative (D) and interchange (I), respectively. Further classification of the interchange pathway as either I_a or I_d is difficult and requires some subjectivity especially since, as discussed below, this rate constant does show a slight dependence on the steric bulk of the Me_nTHF ligand. However, to be consistent with the well established mechanism of other $\text{Cr}(0)$ ligand displacement reactions,³⁰ the k_3 step is classified as a dissociative interchange pathway (I_d). In the case of the k_1 pathway, an intermediate of reduced coordination number is not formed as is required to formally satisfy the definition of a true dissociative mechanism. However, since the Cr – bz bond has to be completely broken before bonding occurs between the Cr center and the entering Me_nTHF ligand, we favor labeling this reaction channel as a dissociative pathway (D).

Assuming that the $\text{Cr}(\text{CO})_5(\text{hep})$ complex is a steady state intermediate, the observed rate can be derived as:

$$k_{\text{obs}} = \frac{k_1 k'' [\text{Me}_n\text{THF}]}{[\text{bz}] + k'' [\text{Me}_n\text{THF}]} + k_3 [\text{Me}_n\text{THF}] \quad (k'' = k_2/k_{-1}) \quad (4)$$

The dependence of k_{obs} on the ligand concentration shown in eqn. (4) is consistent with the experimental observations. Under conditions of low $[\text{Me}_n\text{THF}]$, the observed rate constant will be inversely proportional to the benzene concentration. Also, k_{obs} will exhibit a non-linear dependence on ligand concentration. According to eqn. (4), a plot of the observed rate constant may show curvature with increasing $[\text{Me}_n\text{THF}]$ but depending upon the value of k_3 , the rate constant for the interchange pathway, it may never reach a limiting value. If k_3 is comparable to k_1 , at high ligand concentration k_{obs} might begin to exhibit a linear dependence on $[\text{Me}_n\text{THF}]$. A close look at the experimental data shown in Figs. 3 and 4 suggests that this type of dependence on the ligand concentration may be operative in the case of MeTHF and Me_2THF . The observed rate constant (k_{obs}) appears to saturate but does not reach a limiting value and instead begins to increase linearly with the ligand concentration. This type of superimposed saturation and second order kinetic behavior in the k_{obs} vs. L plots has been observed previously in the reaction kinetics of other organometallic complexes.³¹ When the entering ligand is Me_4THF , however, the k_{obs} vs. $[\text{Me}_4\text{THF}]$ plots appear to saturate at the highest $[\text{Me}_4\text{THF}]$ concentrations implying a minimal contribution from k_3 in this case. Because of the increased steric bulk of the Me_4THF ligand it is reasonable to make the assumption that the transition state for the interchange pathway will be relatively high in energy and that therefore k_3 will not make a significant contribution to the overall mechanism of benzene substitution from $\text{Cr}(\text{CO})_5(\text{bz})$ by Me_4THF . As shown below, this assumption is also justified by the internal consistency of the data.

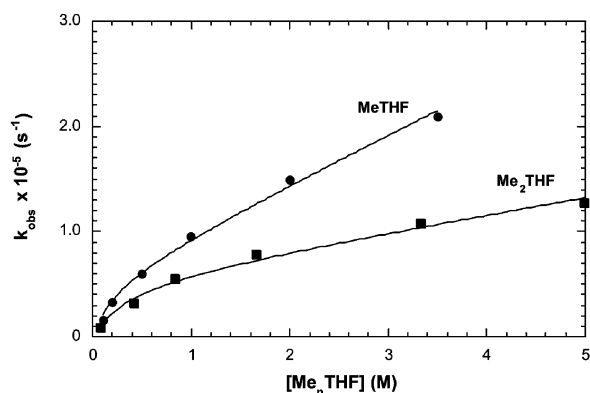


Fig. 4 The solid line shows a fit to the experimental k_{obs} vs. $[\text{Me}_n\text{THF}]$ data obtained at 293 K according to eqn. (4). In these fits the value of k_1 was held constant at $5.67 \times 10^4 \text{ s}^{-1}$ which was determined by studying the reaction of $\text{Cr}(\text{CO})_5\text{bz}$ with Me_4THF at 293 K (see text and Table 1). $[\text{bz}] = 2.8 \text{ M}$.

Making the reasonable assumption that the reaction of the $\text{Cr}(\text{CO})_5(\text{bz})$ complex with Me_4THF proceeds through a dissociative mechanism ($k_3 \approx 0$), then the value of the limiting rate constant will be k_1 , the step associated with the breaking of the $\text{Cr}(\text{CO})_5$ – bz bond. Eqn. (4) may be modified slightly to yield:

$$k_{\text{obs}} = \frac{k_1 k'' [\text{Me}_n\text{THF}]}{[\text{bz}] + k'' [\text{Me}_n\text{THF}]} \quad (k'' = k_2/k_{-1}) \quad (5)$$

Values of k_1 and $k'' (= k_2/k_{-1})$ were obtained from a two parameter non-linear least squares fit of the experimental data according to eqn. (5) (assuming $k_3 = 0$). Two independent runs were conducted and the average values of k_1 and k'' are presented in Table 1. An Eyring analysis using the values of k_1 yields an activation enthalpy of $11.4 \pm 1.1 \text{ kcal mol}^{-1}$ and a $\Delta S_1^\ddagger = +2.2 \pm 3.6 \text{ e.u.}$ According to Scheme 3, k_1 is associated with the breaking of the Cr – bz bond. Thus, the value of $11.4 \pm 1.1 \text{ kcal mol}^{-1}$ is expected to be close to the Cr – bz bond dissociation enthalpy and is in good agreement with the higher estimates of 13.7 ± 0.8 and $14.4 \pm 2.0 \text{ kcal mol}^{-1}$ for the $\text{Cr}(\text{CO})_5$ – bz bond enthalpy obtained from gas phase kinetic studies and PAC, respectively. The agreement between the activation enthalpy presented here and the expected Cr – bz bond enthalpy is consistent with the initial assumption that in the case of Me_4THF , the substitution mechanism follows a primarily dissociative pathway.

The relatively low activation entropy associated with k_1 ($+2.2 \text{ e.u.}$) suggests that the Cr – bz bond is not fully dissociated in the transition state. This observation is consistent with the results of a previous study that indicated some amount of “agostic” Cr – H – C_6H_5 bonding in the transition state associated with the dissociation of benzene from the Cr center.¹⁵ The low value for the activation entropy for this dissociative reaction is also consistent with other studies on similar systems. For example, Dobson has compiled data on 13 $\text{M}(\text{CO})_5(\text{amine})$ [$\text{M} = \text{Cr}, \text{Mo}$] complexes that undergo dissociative substitution of the amine and found that the activation entropies vary from -2 to $+10 \text{ e.u.}$ For weakly binding ligands like benzene and halogenated organics, the ΔS^\ddagger values range from -4 to $+19 \text{ e.u.}$ ³² As discussed later, the low activation entropy is probably due to the fact that the Cr – bz bond continues to dissociate past the transition state.

Analysis of k_3 values

Using the values of k_1 obtained in the case of Me_4THF , the k_{obs} vs. $[\text{Me}_n\text{THF}]$ ($n = 1$ and 2) plots can then be fit according to eqn. (4) to yield an estimate of k_3 and the appropriate k_2/k_{-1} ratios (k''). The results from the fits (Fig. 4) which have R values ≥ 0.98 are shown in Table 2. The data suggest that k_3 makes

Table 1 Rate constants and associated activation parameters for the reaction of (CO)₅Cr(bz) with Me₄THF and THF

Temperature/K	THF ^a $k \times 10^{-4}/\text{M}^{-1} \text{ s}^{-1}$	Me ₄ THF ^b $k_1 \times 10^{-4}/\text{s}^{-1}$ [$k'' (= k_2/k_{-1})$]
293	5.67 ± 0.10	5.67 ± 0.46 [2.8 ± 0.6]
298	6.94 ± 0.11	8.20 ± 0.76 [2.7 ± 0.6]
303	9.31 ± 0.11	11.3 ± 1.0 [2.8 ± 0.6]
308	11.2 ± 0.2	16.0 ± 1.1 [2.8 ± 0.5]
313	13.3 ± 0.7	21.1 ± 1.5 [2.5 ± 0.4]
	$\Delta H_3^\ddagger = 7.5 \pm 0.5 \text{ kcal mol}^{-1}$ $\Delta S_3^\ddagger = -11.4 \pm 1.8 \text{ e.u.}$	$\Delta H_1^\ddagger = 11.4 \pm 1.1 \text{ kcal mol}^{-1}$ $\Delta S_1^\ddagger = +2.2 \pm 3.6 \text{ e.u.}$

^a Values of k obtained from the slope of a plot of k_{obs} vs. [THF]. ^b Values of k_1 and k'' obtained by fitting the plot of k_{obs} vs. [Me₄THF] to eqn. (5) (see text). Note that in the case of Me₄THF, the runs were conducted in mixed solvent with the concentration of [bz] held at 2.8 M. The runs with THF were done in pure benzene solvent. Thus, the rate constants presented in this table are not directly comparable.

Table 2 Rate constants and associated activation parameters for the reaction of Cr(CO)₅(bz) with MeTHF and Me₂THF

Temperature/K	MeTHF ^a $k_3 \times 10^{-4}/\text{M}^{-1} \text{ s}^{-1}$ [$k'' (= k_2/k_{-1})$]	Me ₂ THF ^a $k_3 \times 10^{-4}/\text{M}^{-1} \text{ s}^{-1}$ [$k'' (= k_2/k_{-1})$]
293	5.33 ± 0.22 [9.2 ± 1.9]	1.81 ± 0.19 [7.4 ± 2.9]
298	6.60 ± 0.33 [7.8 ± 1.8]	2.18 ± 0.25 [6.5 ± 2.2]
303	7.96 ± 0.60 [7.3 ± 2.2]	2.68 ± 0.36 [5.9 ± 2.3]
308	—	3.30 ± 0.37 [5.0 ± 1.3]
313	12.1 ± 1.0 [5.8 ± 1.6]	4.33 ± 0.44 [4.5 ± 1.0]
	$\Delta H_3^\ddagger = 6.8 \pm 0.2 \text{ kcal mol}^{-1}$ $\Delta S_3^\ddagger = -13.6 \pm 0.7 \text{ e.u.}$ $\Delta H''^\ddagger = 4.1 \pm 0.5 \text{ kcal mol}^{-1}$ $\Delta S''^\ddagger = -9.6 \pm 1.5 \text{ e.u.}$	$\Delta H_3^\ddagger = 7.3 \pm 0.4 \text{ kcal mol}^{-1}$ $\Delta S_3^\ddagger = -14.2 \pm 1.3 \text{ e.u.}$ $\Delta H''^\ddagger = 4.5 \pm 0.5 \text{ kcal mol}^{-1}$ $\Delta S''^\ddagger = -11.0 \pm 1.5 \text{ e.u.}$

^a Rate constants k_3 and k'' were obtained by fitting the k_{obs} vs. [Me_{*n*}THF] plots to eqn. (4). In these fits, k_1 (presented in Table 1) was held constant at the value determined from a fit to the k_{obs} vs. [Me₄THF] plot (see text).

a significant contribution to the overall rate of benzene substitution in the case of MeTHF and Me₂THF. Notice that according to the mechanism outlined in Scheme 3, the values of k_1 should be insensitive to the nature of the incoming ligand, however, k_3 should show some dependence on the ligand characteristics. Consistent with this expectation, the results show that k_3 is a factor of 3 lower in the case of the more sterically encumbered Me₂THF ligand relative to MeTHF. The k_3 values show a definite temperature dependence and an Eyring analysis (see Fig. 5) yields activation parameters

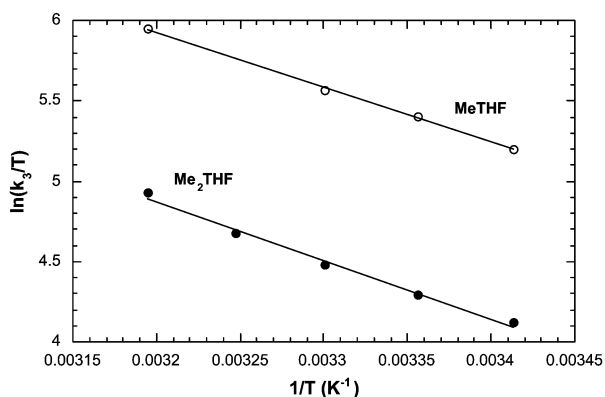


Fig. 5 An Eyring plot of $\ln(k_3/T)$ vs. $1/T$ for MeTHF and Me₂THF: $\Delta H_3^\ddagger = 6.8 \pm 0.2 \text{ kcal mol}^{-1}$, $\Delta S_3^\ddagger = -13.6 \pm 0.7 \text{ e.u.}$ for MeTHF and $\Delta H_3^\ddagger = 7.3 \pm 0.4 \text{ kcal mol}^{-1}$, $\Delta S_3^\ddagger = -14.2 \pm 1.3 \text{ e.u.}$ for Me₂THF.

of $\Delta H_3^\ddagger = 6.8 \pm 0.2 \text{ kcal mol}^{-1}$, $\Delta S_3^\ddagger = -13.6 \pm 0.7 \text{ e.u.}$ when L = MeTHF and $\Delta H_3^\ddagger = 7.3 \pm 0.4 \text{ kcal mol}^{-1}$, $\Delta S_3^\ddagger = -14.2 \pm 1.3 \text{ e.u.}$ when L = Me₂THF. As expected the activation enthalpy associated with k_3 is slightly larger for the bulkier Me₂THF ligand reflecting a greater degree of bond breaking between Cr and benzene before the incoming ligand can be accommodated in the transition state. The significantly negative ΔS_3^\ddagger values reflect the increased order in the transition state as the Me_{*n*}THF ligands begin to bind to the metal center. The ΔH_3^\ddagger values are lower than ΔH_1^\ddagger since the transition state for the k_3 step is expected to be stabilized through residual bonding with benzene and some degree of bond formation with the entering Me_{*n*}THF ligand.

Analysis of $k'' (= k_2/k_{-1})$ values

The values of k_2/k_{-1} obtained from the data analysis for the Me_{*n*}THF ligands also exhibit interesting behavior. This ratio, which represents the relative reactivity of the Cr(CO)₅(hep) intermediate towards benzene and Me_{*n*}THF is expected to decrease, as k_2 decreases, when the Me_{*n*}THF ligand becomes more sterically encumbered. Therefore, the Cr(CO)₅(hep) complex is expected to react faster with MeTHF than with Me₄THF. As shown in Tables 1 and 2, at 298 K, the ratio of k_2/k_{-1} decreases from 9.2 to 2.8 as the entering ligand is varied from MeTHF to Me₄THF. Since k_{-1} is independent of the entering ligand identity, the data suggest that $k_2(\text{MeTHF}) > k_2(\text{Me}_2\text{THF}) > k_2(\text{Me}_4\text{THF})$, consistent with the increasing steric bulk of the Me_{*n*}THF ligand.

The $\text{Cr}(\text{CO})_5(\text{hep})$ complex is moderately selective in its reactions with the entering ligands, reacting almost 10 times faster with MeTHF than with benzene. This observation is also consistent with an earlier study where the substitution of heptane from $\text{Cr}(\text{CO})_5(\text{hep})$ by a variety of ligands was studied.²⁸ The reaction rates were found to be sensitive to the size and electron donating ability of the entering ligand. For example, the $\text{Cr}(\text{CO})_5(\text{hep})$ complex was found to react approximately eight times faster with THF than with 1-hexene.²⁸

In the case of MeTHF and Me₂THF, the k_2/k_{-1} ratios show a temperature dependence and an Eyring analysis (see Fig. 6)

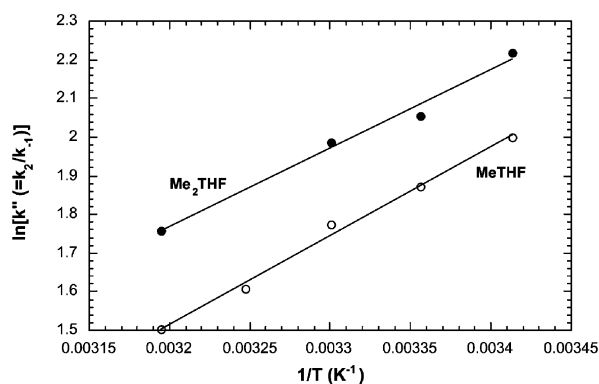


Fig. 6 A plot of $\ln(k'')$ vs. $1/T$. This plot yields the difference in the activation parameters for the reaction of $\text{Cr}(\text{CO})_5(\text{hep})$ with benzene (k_{-1}) and Me_nTHF (k_2): $\Delta H_2^\ddagger - \Delta H_{-1}^\ddagger = -4.1 \pm 0.5 \text{ kcal mol}^{-1}$, $\Delta S_2^\ddagger - \Delta S_{-1}^\ddagger = -9.6 \pm 1.5 \text{ e.u.}$ for MeTHF and $\Delta H_2^\ddagger - \Delta H_{-1}^\ddagger = -4.5 \pm 0.5 \text{ kcal mol}^{-1}$, $\Delta S_2^\ddagger - \Delta S_{-1}^\ddagger = -11.0 \pm 1.5 \text{ e.u.}$ for Me₂THF.

suggests that $\Delta H_2^\ddagger - \Delta H_{-1}^\ddagger = -4.1 \pm 0.5$ and $-4.5 \pm 0.5 \text{ kcal mol}^{-1}$, for MeTHF and Me₂THF respectively. Thus, the activation enthalpy for the reaction of $\text{Cr}(\text{CO})_5(\text{hep})$ with benzene is approximately 4 kcal mol⁻¹ higher than for its reaction with Me₂THF or MeTHF. This result is also consistent with the findings of the earlier study cited above²⁸ which suggested that the activation enthalpy for the reaction between $\text{Cr}(\text{CO})_5(\text{hep})$ and 1-hexene was 3.4 kcal mol⁻¹ higher than for its reaction with THF. Interestingly, this difference in the activation enthalpy is minimized as the steric bulk of the Me_nTHF ligand increases. Thus, the relative temperature independence of the k_2/k_{-1} ratios when the incoming ligand is Me₄THF suggests that there is very little difference in the activation enthalpies associated with the reaction of $\text{Cr}(\text{CO})_5(\text{hep})$ with benzene and Me₄THF. The $\Delta S_2^\ddagger - \Delta S_{-1}^\ddagger$ values are -9.6 ± 1.5 and $-11.0 \pm 1.5 \text{ e.u.}$ for MeTHF and Me₂THF, respectively. These values suggest that there is relatively more Cr–hep bond dissociation in the transition state when $\text{Cr}(\text{CO})_5(\text{hep})$ reacts with benzene than when it reacts with Me₂THF.

Kinetic vs. thermodynamic estimate of Cr–bz bond strength

Previous solution phase kinetic studies estimated an upper limit of 9.4 kcal mol⁻¹ for the Cr–benzene bond strength using piperidine and 1-hexene as the entering ligand.¹⁵ This number was considerably lower than the 14.4 and 13.7 kcal mol⁻¹ estimate for the Cr–benzene bond strength obtained from PAC and gas phase kinetic studies, respectively.^{12,26} In the present case, the $11.4 \pm 1.1 \text{ kcal mol}^{-1}$ value for ΔH_1^\ddagger when L = Me₄THF is in better agreement with the PAC value. While there is some reason to interpret the PAC value with caution since reaction volumes were not taken into account in the bond enthalpy determination,²³ gas phase kinetic studies have also estimated the Cr–bz bond strength to be 13.7 kcal mol⁻¹.¹² The difference of a few kcal mol⁻¹ in the value presented here and the gas

phase and PAC estimates could be due to residual Cr–bz interaction in the transition state associated with k_1 .

Isotope studies involving C₆D₆ have provided strong evidence for residual Cr–H–C₆H₅ “agostic” interaction in the transition state indicating that the “naked” $\text{Cr}(\text{CO})_5$ complex is not generated in the transition state.¹⁵ Thus, the Cr–bz bond may continue to break past the transition state and the resulting increase in enthalpy may be offset by both an increase in entropy and solvation by heptane such that the free energy decreases beyond the transition state as required. In fact, the low activation entropy associated with the k_1 step is consistent with this explanation. Consequently, the kinetic value would underestimate the PAC number by a small amount, as observed. A more complete discussion on the discrepancy between ΔH^\ddagger and ΔH values for other $\text{Cr}(\text{CO})_5$ –solvent bond strength measurements has been presented previously.³²

Energetic profile

Assuming that the “true” $\text{Cr}(\text{CO})_5$ –bz bond dissociation energy is $\approx 14 \text{ kcal mol}^{-1}$ ^{12,26} and the $\text{Cr}(\text{CO})_5$ –hep bond enthalpy measured using PAC is $\approx 11 \text{ kcal mol}^{-1}$,^{26,33} the activation parameters obtained in this study can be put together to yield an enthalpy profile (shown in Fig. 7) for the reaction according

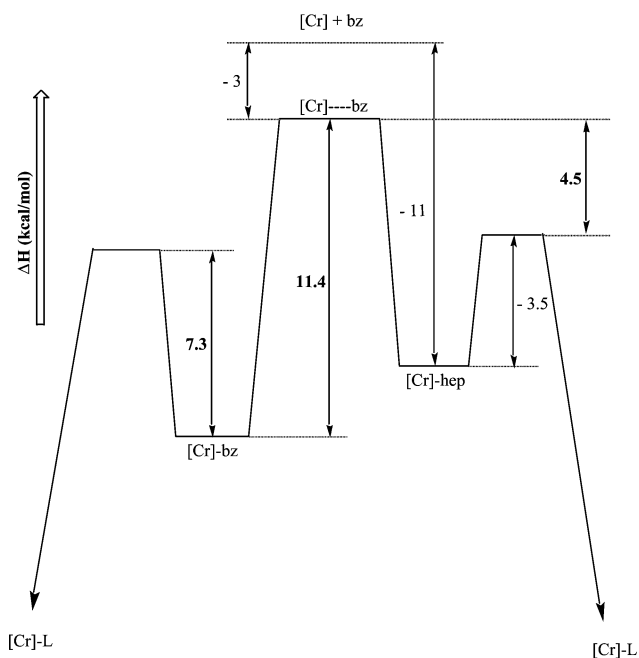


Fig. 7 Enthalpy profile for the reaction of $\text{Cr}(\text{CO})_5(\text{bz})$ with Me₂THF. Here [Cr] = $\text{Cr}(\text{CO})_5$ and L = Me₂THF. Numbers in bold are determined in this study. Other values are estimated from previous work.

to the mechanism shown in Scheme 3. The transition state for the k_1 step is shown to have some residual interaction with benzene resulting in a $\approx 3 \text{ kcal mol}^{-1}$ underestimate of the actual Cr–bz bond enthalpy. The heptane solvent coordinates to the Cr center past this transition state as the Cr–bz bond continues to dissociate to form the $(\text{CO})_5\text{Cr}(\text{hep})$ intermediate. According to this profile, activation enthalpies for the reaction of $\text{Cr}(\text{CO})_5(\text{hep})$ with Me₂THF and benzene are estimated to be 3.5 and 8.0 kcal mol⁻¹, respectively, and are in good agreement with previous studies. Using similar entering ligands, Dobson and co-workers determined activation enthalpies of 4.1 and 7.5 kcal mol⁻¹ for the reaction of $\text{Cr}(\text{CO})_5(\text{hep})$ with THF and 1-hexene, respectively.²⁸ The transition state associated with k_2 is expected to have some amount of Cr–hep interaction since the activation enthalpy for this step is much lower than the thermodynamic estimate of the Cr–hep bond dissociation enthalpy. The overall consistency of the data, internally

and with previous studies, provides good support for the kinetic and mechanistic analysis presented here.

The fair agreement between the thermodynamic (PAC) and kinetic estimate of the $(\text{CO})_5\text{Cr}-(\eta^2\text{-benzene})$ bond strength presented here suggests that the solution phase kinetic method can be useful in determining metal–solvent bond strengths in these systems. However, care must be taken to ensure that the derived activation enthalpies represent the appropriate step in the substitution mechanism and that a sterically encumbered ligand is used to displace the solvent from the metal center so that the transition state has a large degree of metal–solvent dissociation.

Conclusion

The displacement of the benzene solvent from $(\text{CO})_5\text{Cr}(\text{bz})$ by Me_nTHF ($n = 0, 1, 2,$ and 4) ligands has been investigated using the technique of laser flash photolysis. The data presented in this study strongly suggests that the reaction of $\text{Cr}(\text{CO})_5(\text{bz})$ with MeTHF and Me_2THF proceeds through two independent dissociative and interchange (D and I_d) pathways. The contribution of the interchange pathway towards the overall substitution mechanism is progressively minimized as the steric bulk of the entering ligand increases from MeTHF to Me_4THF . Thus, the results are consistent with the assumption that the Me_4THF ligand reacts with $\text{Cr}(\text{CO})_5(\text{bz})$ by a primarily dissociative mechanism while the I_d pathway contributes significantly towards the overall mechanism of benzene substitution by MeTHF and Me_2THF . The data allow us to obtain interesting insights into the energetics of this substitution reaction. The results suggest that the demanding steric factors in the case of the Me_4THF ligand requires significant disruption of the $\text{Cr}–\text{bz}$ bond before the incoming ligand can bond to the Cr center. Thus, the activation enthalpy of $11.4 \pm 1.1 \text{ kcal mol}^{-1}$ obtained for the reaction between $(\text{CO})_5\text{Cr}(\text{bz})$ and Me_4THF is expected to be a lower limit to the $\text{Cr}–\text{benzene}$ bond dissociation enthalpy.

Acknowledgements

The authors would like to thank Dr Richard H. Schultz (Bar-Ilan University, Israel) for helpful discussions.

References

- 1 M. Lee and C. B. Harris, *J. Am. Chem. Soc.*, 1989, **111**, 8963.
- 2 J. D. Simon and K. S. Peters, *Chem. Phys. Lett.*, 1983, **98**, 53.
- 3 L. Wang, X. Zhu and K. G. Spears, *J. Phys. Chem.*, 1989, **93**, 2.
- 4 A. G. Joly and K. F. Nelson, *J. Phys. Chem.*, 1989, **93**, 2876.
- 5 E. Weitz, *J. Phys. Chem.*, 1987, **91**, 3945.
- 6 C. Hall and R. N. Perutz, *Chem. Rev.*, 1996, **96**, 3125.
- 7 J. D. Simon and X. Xie, *J. Phys. Chem.*, 1986, **90**, 6751.
- 8 R. J. Bonneau and J. M. Kelly, *J. Am. Chem. Soc.*, 1980, **102**, 1220.
- 9 S. Wieland and R. van Eldik, *Organometallics*, 1991, **10**, 3110.
- 10 J. P. Collman, L. S. Hegedus, J. R. Norton and P. G. Finke, *Principles and Applications of Organotransition Metal Chemistry*, University Science Books, Mill Valley, CA, 1987.
- 11 P. L. Bogdan, J. R. Wells and E. Weitz, *J. Am. Chem. Soc.*, 1991, **113**, 1294.
- 12 J. R. Wells, P. G. House and E. Weitz, *J. Phys. Chem.*, 1994, **98**, 8343.
- 13 G. R. Dobson, K. J. Asali, C. D. Cate and C. W. Cate, *Inorg. Chem.*, 1991, **30**, 4471.
- 14 S. Zhang and G. R. Dobson, *Organometallics*, 1992, **11**, 2447.
- 15 S. Zhang, G. R. Dobson, V. Zang, H. C. Bajaj and R. van Eldik, *Inorg. Chem.*, 1990, **29**, 3477.
- 16 Y. Ishikawa, C. E. Brown, P. A. Hackett and D. M. Rayner, *Chem. Phys. Lett.*, 1988, **150**, 506.
- 17 P.-F. Yang and G. K. Yang, *J. Am. Chem. Soc.*, 1992, **114**, 6937.
- 18 J. K. Klassen and G. K. Yang, *Organometallics*, 1990, **9**, 874.
- 19 D. M. Hester, J. Sun, A. W. Harper and G. K. Yang, *J. Am. Chem. Soc.*, 1992, **114**, 5234.
- 20 G.-L. Leu and T. J. Burkey, *J. Coord. Chem.*, 1995, **34**, 87.
- 21 J. Morse, G. Parker and T. J. Burkey, *Organometallics*, 1989, **7**, 2471.
- 22 T. Jiao, G.-L. Leu, G. J. Farrell and T. J. Burkey, *J. Am. Chem. Soc.*, 2001, **123**, 4960.
- 23 J. E. Coleman, K. E. Dulaney and A. A. Bengali, *J. Organomet. Chem.*, 1999, **572**, 65.
- 24 S. Ladogana, G. R. Dobson and J. P. Smit, *Inorg. Chim. Acta*, 1998, **271**, 105.
- 25 W. Wang, Y. Zheng, J. Lin, Y. She and K.-J. Fu, *J. Phys. Chem.*, 1993, **97**, 11921.
- 26 T. J. Burkey, *Energetics of Organometallic Species*, J. A. Marinho, ed., Kluwer Academic Publishers, The Netherlands, 1992, pp. 75–94.
- 27 R. Krishnan and R. H. Schultz, *Organometallics*, 2001, **20**, 3314.
- 28 S. Zhang and G. R. Dobson, *J. Coord. Chem.*, 1999, **47**, 409.
- 29 The viscosity of heptane at 298 K is ≈ 0.4 cp while that of benzene is ≈ 0.6 cp.
- 30 D. J. Darensbourg, *Adv. Organomet. Chem.*, 1982, **21**, 113.
- 31 M. J. Wax and R. G. Bergman, *J. Am. Chem. Soc.*, 1981, **103**, 7028.
- 32 S. Ladogana, S. K. Nayak, J. P. Smit and G. R. Dobson, *Inorg. Chem.*, 1997, **36**, 650.
- 33 G. J. Farrell and T. J. Burkey, *J. Photochem. Photobiol. A.*, 2000, **137**, 135.